

See discussions, stats, and author profiles for this publication at: <https://www.researchgate.net/publication/231274695>

Influence of the Surface—Chemistry of Modified Mesoporous Carbon on the Electrochemical Behavior of Solid-State Supercapacitors†

ARTICLE in ENERGY & FUELS · MARCH 2010

Impact Factor: 2.79 · DOI: 10.1021/ef901447y

CITATIONS

20

READS

50

2 AUTHORS:



[Francesco Lufrano](#)

Italian National Research Council

46 PUBLICATIONS 1,813 CITATIONS

[SEE PROFILE](#)



[Pietro Staiti](#)

Italian National Research Council

62 PUBLICATIONS 1,923 CITATIONS

[SEE PROFILE](#)

Influence of the Surface—Chemistry of Modified Mesoporous Carbon on the Electrochemical Behavior of Solid-State Supercapacitors[†]

F. Lufrano* and P. Staiti

CNR-ITAE, Consiglio Nazionale delle Ricerche—Istituto di Tecnologie Avanzate per l'Energia “Nicola Giordano”,
Via Salita S. Lucia sopra Contesse, 5, 98126 Messina, Italy

Received November 30, 2009. Revised Manuscript Received March 3, 2010

This paper reports on the synthesis of the mesoporous CMK-3 carbon carried out using the SBA-15 silica as a template and its chemical modification by nitric acid treatment at room temperature. The nitric-acid-modified carbon, CMK-3AN, was used to prepare other carbon samples by thermal treatments at 700 and 900 °C, which modify the surface properties of carbons by a partial removal of oxygenated surface groups. A series of composite electrodes was prepared from modified and unmodified carbons and used as the active material for solid-state supercapacitors. The electrochemical study carried out in two electrode configurations showed that the insertion of oxygen-containing functional groups in template carbon imparted changing on the capacitance features, enhancing also the electrode/electrolyte interface. However, the one disadvantage of acid treatment was that the carbon and electrodes showed a slight higher electronic resistance. The nitric-acid-modified carbon electrodes (CMK-3AN) showed better capacitive performances (162 F g^{-1} ; on the basis of the weight of the active carbon materials for one electrode) than those of the untreated CMK-3 carbon (132 F g^{-1}) and much higher values than the carbon samples treated at 700 °C (CMK-3AN7) and 900 °C (CMK-3AN9), which showed values of 82 and 49 F g^{-1} , respectively. The high total capacitance of the former carbon originates from its higher pseudo-capacitance, which derived from the presence of electrochemically active oxygen-containing functional groups. These groups were partially eliminated during the thermal treatments at 700 and 900 °C. As a consequence to this, the supercapacitor using the carbon treated at the highest temperature (CMK-3AN9) showed a specific capacitance of about 250% lower than that with the nitric-acid-treated carbon (CMK-3AN).

1. Introduction

Supercapacitors are well-known energy storage devices that deliver high power and store remarkable energy. Even if their stored energy is lower than that of lithium batteries, they can be charged and discharged for hundreds of thousands cycles without adversely affecting their lifetime; it is known that batteries suffer from a low cycling life (generally < 1000). Generally, the active materials in electrochemical supercapacitors are activated carbons and/or carbon fibers, in which the mechanism of storing the electric charge is mainly capacitive because it occurs by the formation of an electric double layer on the carbon surface. There are also types of supercapacitors that involve chemical reactions in the energy storage mechanism by means of the faradaic process (redox process), which is

generally based on metal oxides, such as RuO_x , NiO_x , and MnO_2 ,^{1–5} and electronically conducting polymers (ECPs).^{6,7}

However, a faradaic capacitance can also be achieved with carbon materials containing electrochemically active surface functional groups, although these functionalized carbons provide a smaller amount of pseudo-capacitance than inorganic metal oxide materials.

Nevertheless, their easy preparation process through the chemical modification (oxidation) of the surface of the carbon makes such modifications interesting. The influence of functional species on carbon material properties has been investigated for many decades to improve the adsorption and separation properties^{8,9} and/or the adsorption and removal of metal ions^{10,11} and to increase the specific capacitance and hydrophilic properties of carbon-material-based supercapacitors.^{12,13}

[†] This paper has been designated for the special section Carbon for Energy Storage and Environment Protection.

* To whom correspondence should be addressed. E-mail: lufrano@itaec.cnr.it.

(1) Conway, B. E. *Electrochemical Supercapacitors: Scientific Fundamental and Technological Applications*; Kluwer Academic/Plenum Publishers: New York, 1999.

(2) Burke, A. *Electrochim. Acta* **2007**, *53*, 1083–1091.

(3) Simon, P.; Gogotsi, Y. *Nat. Mater.* **2008**, *7*, 845–854.

(4) Toupin, M.; Brousse, T.; Belanger, D. *Chem. Mater.* **2004**, *16*, 3184–3190.

(5) Khomenko, V.; Raymundo-Pinero, E.; Beguin, F. *J. Power Sources* **2006**, *153*, 183–190.

(6) Arbibzani, C.; Mastragostino, M.; Soavi, F. *J. Power Sources* **2001**, *100*, 164–170.

(7) Laforgue, A.; Simon, P.; Fauvarque, J. F.; Mastragostino, M.; Soavi, F.; Sarrau, J. F.; Lailler, P.; Conte, M.; Rossi, E.; Saguatti, S. *J. Electrochem. Soc.* **2003**, *150*, A645–A651.

(8) Radovic, L. R.; Moreno-Castilla, C.; Rivera-Utrilla, J. Carbon materials as adsorbents in aqueous solutions. In *Chemistry and Physics of Carbon*; Radovic, L. R., Ed.; Marcel Dekker: New York, 2001; Vol. 27, pp 227–405.

(9) Celzard, A.; Fierro, V. *Energy Fuels* **2005**, *19*, 573–583.

(10) Xiao, B.; Thomas, K. M. *Langmuir* **2004**, *20*, 4566–4578.

(11) Rodriguez-Reinoso, F.; Sepulveva-Escribano, A. In *Carbon Materials for Catalyst*; Serp, P.; Figueredo, J. L., Eds.; Wiley–Blackwell: Oxford, U.K., 2009; pp 131–156.

(12) Lozano-Castello, D.; Cazorla-Amoros, D.; Linares-Solano, A.; Shiraiishi, S.; Kurihara, H.; Oya, A. *Carbon* **2003**, *41*, 1765–1775.

(13) Frackowiak, E.; Beguin, F. *Carbon* **2001**, *39*, 937–950.

Ordered mesoporous carbons are a new and interesting type of carbonaceous material with an excellent potential in energy storage technologies because of the possibilities for use as the negative electrode material of the lithium battery^{14,15} and as the capacitive material in electrochemical supercapacitors.^{16–18} It is well-known that ionic species are hindered at a high rate performance when the carbon materials contain a large fraction of small micropores. Instead, if carbon materials are based on mesopores, a higher surface use than in microporous carbons can be achieved. In this work, we report on the preparation of mesoporous carbon materials with a hexagonal structure (*P6mm*) of type CMK-3 obtained using the SBA-15 silica template.

The CMK-3 carbon was modified by treatment with nitric acid by inserting oxygen-containing functional groups on the surface, which changed the hydrophobic/hydrophilic properties of the material. Recently, we demonstrated that solid-state supercapacitors based on the Nafion electrolyte with a high specific capacitance can be efficiently realized.^{19,20} A high specific capacitance of 130 F g⁻¹ (on the basis of the carbon material for a single electrode) was reported in a 4 cm² supercapacitor,¹⁹ and a specific capacitance of 114 F g⁻¹ was also obtained for a prototype of a supercapacitor of 1.5 F and 5 V.²⁰

In our studies, a high ionic conductivity of 6×10^{-2} S cm⁻¹ at room temperature in a solid-state supercapacitor with a flexible configuration was shown. Because Nafion is well-known as a hydrophilic material because it bears sulfonic groups on a backbone structure, it is likely that its mixing is improved with carbon materials containing functional groups.

Hence, starting from these considerations, here, we report the synthesis and chemical modification of a CMK-3 carbon and its use in the preparation of composite electrodes for electrochemical supercapacitors. The hydrophilic/hydrophobic properties of different mesoporous carbons obtained after chemical modification with nitric acid and successive thermal treatments were studied and used for the comparison of carbon-based electrodes in 4 cm² solid-state supercapacitors.

2. Experimental Section

2.1. Synthesis of SBA-15 Silica. The preparation of the mesoporous carbons was carried out through the preliminary preparation of a silica template. The silica SBA-15 was synthesized by a procedure similar to that reported by Zhao et al.²¹ In a typical synthesis procedure, 20 g of the triblock copolymer of poly(ethylene glycol)₂₀-block-poly(propylene glycol)₇₀-block-poly(ethylene glycol)₂₀ (EO₂₀PO₇₀EO₂₀) (average MW = 5800, Aldrich) was dispersed in 150 mL of H₂O, followed by the addition of 580 mL of 2 M HCl. The solution was stirred at 35 °C in a three-necked round-bottom flask until complete polymer dissolution and a clear solution was obtained. Afterward,

- (14) Zhou, H.; Zhu, S.; Hibino, M.; Honma, I.; Ichihara, M. *Adv. Mater.* **2003**, *15*, 2107–2111.
- (15) Fan, J.; Wang, T.; Yu, C.; Tu, B.; Jiang, Z.; Zhao, D. *Adv. Mater.* **2004**, *16*, 1432–1436.
- (16) Fuertes, A. B.; Pico, F.; Rojo, J. M. *J. Power Sources* **2004**, *133*, 329–336.
- (17) Centeno, T. A.; Sevilla, M.; Fuertes, A. B.; Stoeckli, F. *Carbon* **2005**, *43*, 3002–3039.
- (18) Xing, W.; Qiao, S. Z.; Ding, R. G.; Li, F.; Lu, G. Q.; Fan, Z. F.; Cheng, H. M. *Carbon* **2006**, *44*, 216–224.
- (19) Lufrano, F.; Staiti, P. *Electrochim. Acta* **2004**, *49*, 2683–2689.
- (20) Staiti, P.; Lufrano, F. *J. Electrochem. Soc.* **2005**, *152*, A617–A621.
- (21) Zhao, D.; Feng, J.; Huo, Q.; Melosh, N.; Fredrickson, G. H.; Chemka, B. F.; Stucky, D. G. *Science* **1998**, *279*, 548–552.

43.4 g of tetraethoxysilane (TEOS) was added under continuous stirring at 35 °C, and these conditions were maintained for 20 h. After the stirring was stopped, a hydrothermal treatment at 100 °C for 24 h was carried out. The product was finally filtered, dried at ambient temperature, and calcined in air at 500 °C for 6 h.

2.2. Synthesis of Mesoporous CMK-3 Carbon. Mesoporous carbons were prepared by the silica SBA-15 following the procedure described by Jun et al.²² In a typical synthesis procedure, 30 g of H₂O, 0.86 g of concentrated H₂SO₄, and 7.65 g of sucrose were homogenized in a beaker by stirring. The dispersion was added drop by drop to 6.02 g of the SBA-15 silica on the bottom of a glass beaker. The impregnated silica sample was first heated in an oven at 100 °C for 6 h and, afterward, at 160 °C for 6 h. This latter step was repeated a second time, adding a lower amount of sucrose: 30 g of H₂O, 0.54 g of H₂SO₄, and 4.8 g of sucrose. After the thermal treatment at 160 °C, the materials were pyrolyzed in a quartz tube under inert helium at 850 °C. Finally, the silica template was removed by treating with 1.5 M NaOH solution (50 vol % ethanol/50 vol % H₂O) at 70 °C. The carbon sample pyrolyzed at 850 °C was designed as CMK-3.

2.3. Chemical and Thermal Modification of Mesoporous CMK-3 Carbon. The acid treatment of CMK-3 carbon was carried out with 70% nitric acid solution for 3 h at room temperature. The suspension was then leached with 10 times the amount of distilled water and decanted overnight. The sediment, separated from the acid solution, was washed with hot distilled water to be sure that the nitric acid had been eliminated. Finally, the powder was dried at 130 °C for 3 h. The nitric-acid-modified carbon, CMK-3AN, was divided into three samples: the first, CMK-3AN, was left unmodified, while other two samples were thermal-treated in a quartz tube in flowing helium at 700 °C (CMK-3AN7) and 900 °C (CMK-3AN9). The four samples were used to prepare electrodes, which were studied in small-size solid-state supercapacitors.

2.4. Physical–Chemical Characterization of Mesoporous Carbons. Low-temperature nitrogen adsorption/desorption measurements were performed at 77 K with a Sorptomatic (mod. 1990) (ThermoQuest, Milan, Italy). Before the measurements, the carbon and the electrode samples were degassed at 250 °C in high vacuum for at least 3 h.

The specific surface area of different samples was determined by the Brunauer–Emmett–Teller (BET) method in the P/P_0 range from 0.05 to 0.25, whereas the total pore volume was calculated at a relative pressure of $P/P_0 = 0.95$. A comparative αS plot was used for the assessment the total specific surface area (S_{tot}), which is based on the comparison of the adsorption isotherm of the studied carbon with the standard isotherm of a reference nonporous carbon black, Cabot BP 280.²³

The surface area and the volumes of the mesopores as well as their pore size distributions (PSDs) were evaluated from the desorption branch of the isotherms using the Barrett–Joyner–Halenda (BJH) method,²⁴ considering the International Union of Pure and Applied Chemistry (IUPAC) mesopore range from 50 to 2 nm.

The Dubinin–Radushkevich theory was used to determine the micropore volume, V_{mi} (pore size smaller than 2 nm), and the corresponding micropore surface area (S_{mi}) was obtained by the Dubinin–Kaganer (DR) method. The DR method was also used to estimate the average micropore width (L_0) assuming that locally the pores are slit-shaped. The L_0 is calculated with the simple relation L_0 (nm) = V_{mi} (cm³ g⁻¹) × 2000/ S_{mi} (m² g⁻¹).^{25,26}

- (22) Jun, S.; Joo, S. H.; Ryoo, R.; Kruk, M.; Jaroniec, M.; Liu, Z.; Ohsuna, T.; Terasaki, O. *J. Am. Chem. Soc.* **2000**, *122*, 10712–10713.

- (23) Kruk, M.; Jaroniec, M.; Choma, J. *J. Colloid Interface Sci.* **1997**, *192*, 250.

- (24) Barrett, E. P.; Joyner, L. G.; Halenda, P. P. *J. Am. Chem. Soc.* **1951**, *73*, 373.

- (25) Stoeckli, F.; Centeno, T. A. *Carbon* **2005**, *43*, 1184–1190.

- (26) Centeno, T. A.; Stoeckli, F. *Electrochim. Acta* **2006**, *52*, 560–566.

The porous properties were analyzed using the Advanced Data Processing version 5.1 software by Thermo Electron.

Powder X-ray diffraction measurements were performed using a Philips X'Pert Pro diffractometer using Cu K α radiation (wavelength = 0.15418 nm), whereas transmission electron microscope (TEM) images were collected by a Philips CM12 instrument.

X-ray photoelectron spectroscopy (XPS) analysis was used to determine the oxygen-containing functional groups present on the surface of carbon samples. This analysis was performed using a Physical Electronics (PHI) 5800-01 spectrometer. Spectra were obtained with pass energies of 58.7 eV for elemental analysis and 11.75 eV for the determination of the oxidation states and chemical compositions. The analysis chamber pressure was lower than 10^{-9} Torr.

To determine the elemental surface composition, a survey scan was used. The survey scan was obtained by generating a spectrum from 0 to approximately 1200 eV for the whole spectra (0–1200 eV), and narrow ones at high resolution for the elements (C 1s, O 1s, and N 1s) were also recorded. Mass percentages of the surface groups were determined by integrating the area under the peaks. The binding energy scale was regulated by setting the C 1s transition at 284.6 eV. Peak areas were estimated by calculating the integral of each peak after subtraction of the background and fitting the experimental peak by a Gaussian curve.

2.5. Preparation of the Composite Electrodes. The electrodes for the supercapacitor were prepared using a casting method, which consisted of spreading a slurry of the carbon material, Nafion ionomer, graphite fibers, and solvent *N,N*-dimethylacetamide (DMAc) on a glass plate. After the casting process, the electrodes were treated at 120 °C for 1 h and 160 °C for 20 min. The composition of the prepared self-supported electrodes was 45 wt % carbon, 50 wt % Nafion, and 5 wt % graphite fibers. The carbon loading in the studied four different electrodes was 4.7, 6.6, 6.1, and 6.57 for CMK-3, CMK-3AN, CMK-3AN7, and CMK-3AN9, respectively.

2.6. Electrochemical Characterization of Carbon-Based Solid-State Supercapacitors. The membrane electrode assemblies (MEAs) for supercapacitor testings were obtained by contacting face-to-face two 4 cm² electrodes with a 5 cm² Nafion 115 membrane (DuPont). The assemblies were completed by a hot pressing procedure at 100 kg/cm² and 130 °C for 10 min.

The electrochemical characterization on a 4 cm² complete supercapacitor was performed by cyclic voltammetry (CV) at different voltage sweep rates from 5 to 40 mV/s and galvanostatic charge/discharge measurements in the voltage window of 0–1 V at current densities from 1.25 to 10 mA cm⁻², using AMEL equipment (Amel srl, Milan, Italy). The electrochemical impedance spectroscopy (EIS) measurements were performed by a Potentiostat PGSTAT 30 (Autolab, Eco Chemie, Utrecht, The Netherlands) with a FRA2 module at frequencies from 1 mHz to 10 MHz.

3. Results and Discussion

3.1. Physical and Chemical Characterization of Mesoporous Carbons. The porous structure of the prepared carbons was determined by nitrogen adsorption measurements. Figure 1 shows the nitrogen adsorption–desorption isotherms of mesoporous CMK-3 carbon and the carbon electrodes CMK-3 EL, CMK-3AN EL (CMK-3 carbon treated with nitric acid), CMK-3AN7 EL (CMK-3AN thermally treated at 700 °C), and CMK-3AN9 EL (CMK-3AN thermally treated at 900 °C). The isotherms of the carbon and electrodes were type-IV curves with a capillary condensation step and a slight hysteresis loop at relative pressures (P/P_0) higher than 0.45, which is indicative of mesoporosity. The high N₂ sorption at low ratio P/P_0 for all studied carbon and

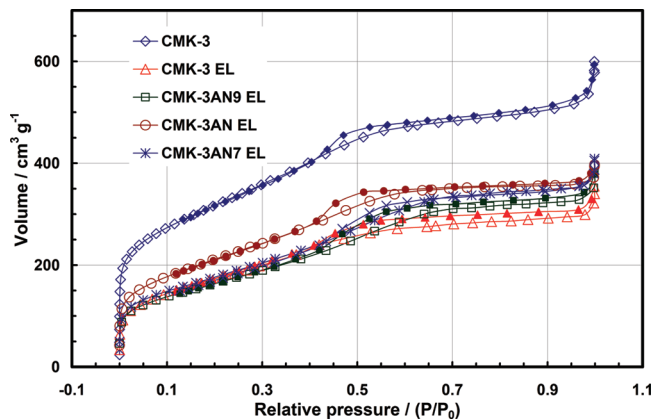


Figure 1. Nitrogen adsorption and desorption of the CMK-3 carbon and carbon electrodes.

electrode materials indicates that these carbons are also microporous. The DR micropore volume (V_{mi}) was 0.41, 0.22, 0.29, 0.21, and 0.22 cm³ g⁻¹ for CMK-3, CMK-3 EL, CMK-3AN EL, CMK-3AN7 EL, and CMK-3AN9 EL, respectively. The specific surface area, pore volume, and other textural properties of the carbons and electrode are summarized in Table 1. The BET specific surface areas of the mesoporous carbons were 1120, 633, 766, 623, and 594 m² g⁻¹ for CMK-3, CMK-3 EL, CMK-3AN EL, CMK-3AN7 EL, and CMK-3AN9 EL, respectively, whereas the total pore volumes at $P/P_0 = 0.95$ were 0.80, 0.46, 0.55, 0.51, and 0.51 cm³ g⁻¹ for the same materials. The analysis of isotherms also showed a difference of about 40% of BET specific surface area between the CMK-3 EL (electrode) and carbon powder (CMK-3), i.e., 633 versus 1120, which is because of the Nafion binder that covers a great number of pores in the electrode.

Figure 2 shows the PSD (BJH) of studied materials. The PSD shows similar mesopore distributions and average pore diameters (BJH) between 3.45 and 3.61 nm, with a variation of pore diameters of less than 5%. A high volume of desorbed nitrogen (cm³ g⁻¹) in the PSD (Figure 2) for diameters from 1.5 to 3 nm and similar slopes in the isotherms of carbon electrodes (Figure 1) at relative pressure (P/P_0) from 0.1 to 0.35 indicate the presence of supermicropores and small mesopores in these electrodes. The presence of micropores in these template carbons were likely originated from the carbonization process of the sucrose and should be localized inside the carbon rods and/or the spacers that connect the carbon rods, in agreement with that reported in the literature.^{27,28} The changing in the microporosity/mesoporosity ratio of different carbons indicated that acid and thermal treatments produced slight structural rearrangement. The values of the volume of microporosity shown in Table 1 are in the range of 0.21–0.41 cm³ g⁻¹, comparable to those previously reported by other authors^{22,27–29} for the same type of carbon (CMK-3). The micropore width (L_0) was found to be 0.77, 0.74, 0.73, 0.72, and 0.71 nm for CMK-3, CMK-3 EL, CMK-3AN EL, CMK-3AN7 EL, and CMK-3AN9 EL, respectively, which indicate very similar micropore characteristics.

(27) Vix-Guterl, C.; Frackowiak, E.; Jurewicz, K.; Fribe, M.; Parmentier, J.; Beguin, F. *Carbon* **2005**, *43*, 1293–1302.

(28) Xia, K.; Gao, Q.; Jiang, J.; Hu, J. *Carbon* **2008**, *46*, 1718–1726.

(29) Kim, D. J.; Lee, H. I.; Yie, J. E.; Kim, S. J.; Kim, J. M. *Carbon* **2005**, *43*, 1868–1873.

Table 1. Textural Properties of Mesoporous Carbon and Electrodes

sample	S_{BET}^a ($\text{m}^2 \text{ g}^{-1}$)	S_{tot}, α_S ($\text{m}^2 \text{ g}^{-1}$)	$S_{\text{mi}}^{\text{DR}}$ ($\text{m}^2 \text{ g}^{-1}$)	$S_{\text{ext}}^{\text{as}}$ ($\text{m}^2 \text{ g}^{-1}$)	V_p^b ($\text{cm}^3 \text{ g}^{-1}$)	V_{mi}^c ($\text{cm}^3 \text{ g}^{-1}$)	D_p (nm) BJH ^d	L_0 (nm) ^e
CMK-3	1120	1110	1070	88	0.80	0.41	3.53	0.77
CMK-3 EL	633	717	591	36	0.46	0.22	3.45	0.74
CMK-3AN EL	766	827	790	32	0.55	0.29	3.51	0.73
CMK-3AN7 EL	623	645	580	37	0.51	0.21	3.59	0.72
CMK-3AN9 EL	594	645	623	44	0.51	0.22	3.61	0.71

^a Specific surface area determined by the BET method for P/P_0 from 0.05 to 0.25. ^b Total pore volume calculated at $P/P_0 = 0.95$. ^c Volume of micropores (V_{mi}) (<2 nm) as determined by Dubinin–Radushkevich. ^d Pores diameter (D_p) as determined by BJH from desorption data. ^e Micropore width (L_0) as determined by V_{mi} ($\text{cm}^3 \text{ g}^{-1}$) = L_0 (nm) × S_{mi} ($\text{m}^2 \text{ g}^{-1}$) / 2000.

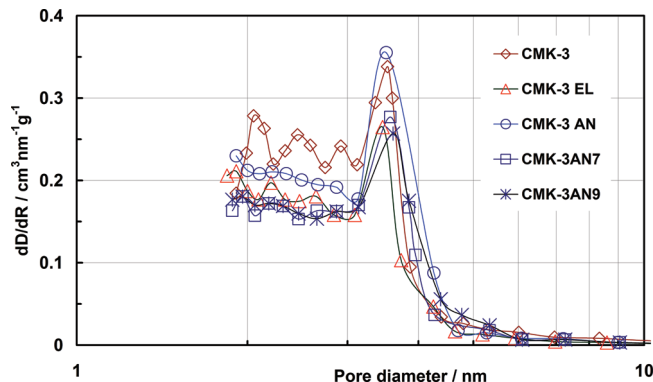


Figure 2. Mesopore size distribution (BJH) of the CMK-3 carbon and carbon electrodes.

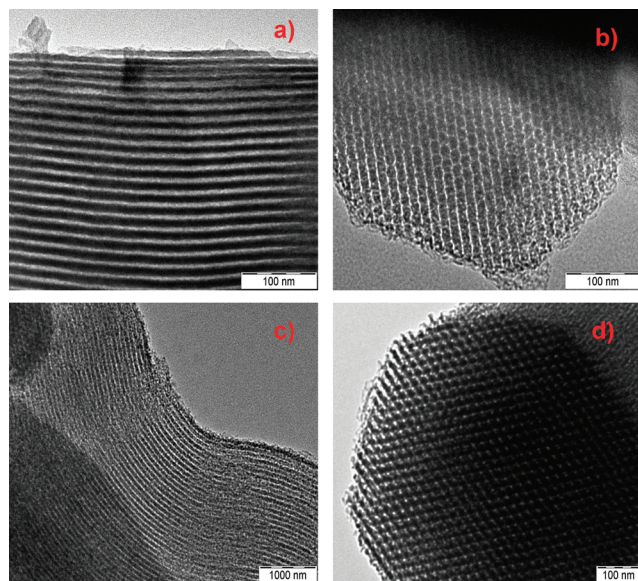


Figure 3. TEM images of SBA-15 and the CMK-3 carbon: (a) lateral view of channels of a particle of SBA-15, (b) frontal view of SBA-15 channels, (c) lateral view of the CMK-3 carbon channels, and (d) frontal view of the CMK-3 carbon channels.

Figure 3 shows the TEM images of channels for the synthesized silica (SBA-15) and the CMK-3 carbon. Figure 3a provides evidence of the characteristic structure of the silica SBA-15 with the channels in a hexagonal arrangement. Figure 3b shows the structure of the silica from the frontal view of the channels. The interchannel distances for SBA-15 measured from the image are about 9 nm. Panels c and d of Figure 3 show the structure of the CMK-3 carbon. From the latter carbon TEM image, the hexagonal structure of the material is apparent, with average diameters for the carbon rods of approximately 7 nm and an interaxis distance

between the two adjacent carbon rods of ~8.5 nm. These values are in agreement with those reported by Jun et al.²² The highly ordered structure of the synthesized silica SBA-15 template and the mesoporous CMK-3 carbons was also confirmed by small-angle XRD analyses (not reported here). The presence of peaks in the XRD patterns at low angles might be assigned to (100), (110), and (200) diffractions from the 2D symmetry associated with the hexagonal structure. The calculated value of d spacing was 8.25 nm for the CMK-3 carbon, in agreement with those measured by TEM micrographs.

Table 2 reports the composition obtained by XPS analysis of treated and untreated carbon samples on the basis of the different content of carbon, oxygen, and nitrogen elements. The high-resolution C 1s and O 1s spectra reveal the presence of several peaks of oxygen-containing functional groups introduced from the nitric acid treatment. A partial removal of these groups was obtained by successive thermal treatments at 700 and 900 °C.

The ratio of $O_{\text{tot}}/C_{\text{tot}}$ reported in Table 2 indicates the degree of surface oxidation of acid- and thermal-treated carbons. High-resolution XPS spectra of the C 1s region (Table 2a) show that carbon-based oxides present on the analyzed samples are also included on the unmodified CMK-3 carbon. Deconvolution of the C 1s spectra gives five peaks:^{30–32} peak 1 (284.3 ± 0.1 eV) corresponds to the graphitic carbon of hybridation sp²; a second peak (peak 2) at 284.6 ± 0.1 eV should be due to distortion of hybridation sp²,³¹ peak 3 (286.2 ± 0.4 eV) is generally assigned to carbon from phenols and ethers; peak 4 (288 ± 0.1 eV) is due to carbonyl or quinone groups; and peak 5 (290.3 ± 0.1 eV) is for carboxyl or ester groups. The O 1s spectra are usefully deconvoluted into four peaks: peak I (530.2 ± 0.2 eV) corresponds to quinone (C=O) groups; peak II (531.2 ± 0.2 eV) corresponds to carbonyl (C=O) from anhydrides and lactones and COH from phenols; peak III (532.6 ± 0.2 eV) corresponds to oxygen from ethers (–CO–O–R); and peak IV (534 ± 1 eV) corresponds to oxygen from carboxyl groups and/or adsorbed water. The nitric-acid-treated sample (CMK-3AN) is the carbon with the higher oxygen content, 9.17 atomic %, whereas the unmodified CMK-3 carbon has 6.11 atomic %, and the two thermal treated samples contain 3.66 and 4.11 atomic % for CMK-3AN7 and CMK-3AN9, respectively. Analyzing the data of Table 2, it is found that the carbons contain similar oxygenated groups on the surface even if the oxygen content in the whole carbons is different for the chemical- and thermal-treated carbons (from 9.17 to

(30) Zhou, J.-H.; Sui, Z.-J.; Zhu, J.; Li, P.; Chen, D.; Dai, Y.-C.; Yuan, W.-K. *Carbon* **2007**, *45*, 785.

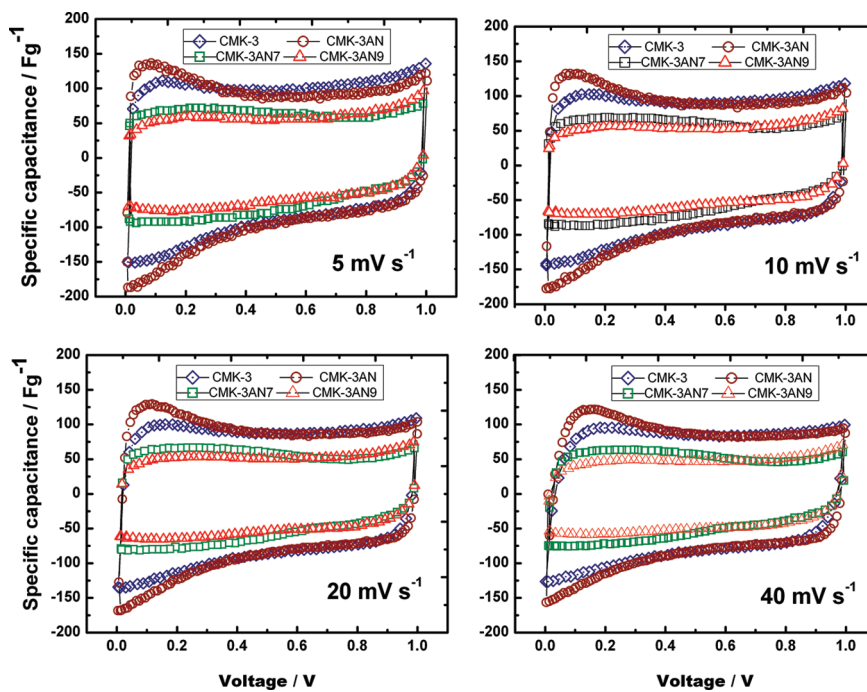
(31) Larciprete, R.; Gardonio, S.; Petaccia, L.; Lizzit, S. *Carbon* **2009**, *47*, 2579.

(32) Yue, Z. R.; Jiang, W.; Wang, L.; Gardner, S. D.; Pittman, C. U. *Carbon* **1999**, *37*, 1785.

Table 2. Contents of C 1s and O 1s and Assignment for the C 1s and O 1s Components from XPS Spectra

(a) Contents of C 1s and O 1s and Assignment for the C1s Components from XPS Spectra								
			C1	C2	C3	C4	C5	
BE (eV)			284.3	284.6	286.2	288.0	290.2	
sample	C 1s (%)	O 1s (%)	$O_{\text{tot}}/C_{\text{tot}}$	C–C sp2	C–C sp2	C–OH C–O–R	C=O quinones	COOR COOH
CMK-3	92.55	6.11	0.066	48.32	25.05	12.83	5.62	8.18
CMK-3AN	90.14	9.17	0.102	44.59	30.00	8.98	6.96	9.46
CMK-3AN7	96.47	3.66	0.038	40.52	28.34	15.33	5.63	10.17
CMK-3AN9	95.6	4.11	0.043	47.24	24.36	13.11	4.76	10.53

(b) Contents of C 1s and O 1s and Assignment for the O1s Components from XPS Spectra								
			O1	O2	O3	O4	O5	
BE (eV)			530.2	531.2	532.6	534.1	535.0	
sample	C 1s (%)	O 1s (%)	$O_{\text{tot}}/C_{\text{tot}}$	C=O quinones	C=O anhydrides	C–OH	ether oxygen	CO–O–R
CMK-3	92.55	6.11	0.066	3.50	14.83		56.78	24.00
CMK-3AN	90.14	9.17	0.102	4.49	9.99		61.62	23.67
CMK-3AN7	96.47	3.66	0.038	10.04	10.93		53.49	25.27
CMK-3AN9	95.6	4.11	0.043	4.19	12.32		58.60	24.89
								0.00
								water

**Figure 4.** Characteristic specific capacitance versus potential of the different CMK-3 carbon-based supercapacitors at various sweep rates: 5, 10, 20, and 40 mV s^{-1} .

3.66 atomic %). The XPS analysis of modified carbons shows the presence of a small content of nitrogen functional groups, which vary from 0.69% for CMK-3AN carbon to 0.29% for CMK-3AN7 and CMK-3AN9 carbons.

3.2. CV Studies on Carbon Materials. Figure 4 shows the capacitance behavior of the different carbon-based supercapacitors at different voltage sweep rates from 5 to 40 mV s^{-1} . The data of the figure report the specific capacitance, calculated for one electrode, as a function of the voltage. The original values of current of the CV were converted in capacitance for one electrode by the relation $C(\text{F g}^{-1}) = [(I(\text{A})/\text{d}V\text{d}t^{-1} (\text{V s}^{-1})]/\text{mass}_{\text{capacitor}} (\text{g}) \times 4$. The curves indicate that the supercapacitor with the CMK-3AN carbon (nitric-acid-modified carbon) exhibits a higher specific capacitance

than those with the untreated CMK-3 carbon and thermal-treated carbons CMK-3AN7 and CMK-3AN9, notwithstanding that these latter carbons show more rectangular shapes in the voltammetric diagrams. The voltammograms of the CMK-3AN carbon show a peak in the voltage range of 0–0.3 V during charging and an increase in the negative current during discharging from 0.3 to 0 V at all voltage sweep rates. The shapes of these curves are different from that of the pure capacitive capacitor, which presents a box-like shape. This behavior is also shown by the CMK-3 carbon, even if it is less apparent compared to CMK-3AN. The voltammetric behavior of these carbon-based supercapacitors indicates the presence of a remarkable pseudo-capacitance together with a double-layer capacitance. As shown in the

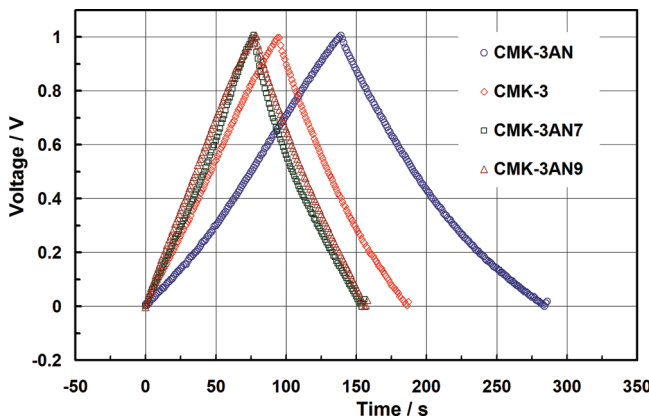


Figure 5. Galvanostatic charge and discharge measurements of different template carbon-based supercapacitors. Current density = 2.5 mA cm^{-2} .

XPS analysis, the carbons contain on their surface different oxygen-containing functional groups that can be active to provide pseudo-capacitance by the redox process. The quinones might be some of these groups because of the well-known quinone–hydroquinone equilibrium: $\text{Q} + 2\text{H}^+ + 2e^- = \text{QH}_2$, which might supply a pseudo-capacitance for 2 eV for a quinone group, whereas the equivalent double-layer capacitance can reach only 0.18 eV.^{1,33} Hence, even with a little content of quinone groups, a remarkable capacitance from faradaic processes can be obtained. A confirmation of the content of quinone groups in these studied carbons was obtained on the analysis of O 1s spectra reported in Table 2b. The binding energy of $530.2 \pm 0.2 \text{ eV}$ is unequivocally assigned at quinone groups, whereas the band at $531.2 \pm 0.2 \text{ eV}$ is assigned at other carbonyl oxygen groups, such as anhydrides and lactones. The CMK-3AN7 is the carbon with a higher content of quinone-type groups (10 atomic %) compared to other carbons, but it has a lower content of oxygen. Other oxygen-containing functional groups, which include carboxyl groups, lactones, hydroxyl carbonyl, phenols, and pyrones, could be electrochemically active on carbon surfaces at potentials lower than 0.6–0.7 V versus the normal hydrogen electrode (NHE).^{34,35} The pseudo-capacitance obtainable from these functionalities is not well-demonstrated in the literature, but it cannot be excluded. However, it is expected that oxygenated groups modify the electronic resistance of carbon and, therefore, influence the electrochemical properties.

3.3. Galvanostatic Charge and Discharge Measurements of Different Carbons. Galvanostatic charge/discharge measurements were used to highlight the capacitance characteristic of carbon-based solid-state supercapacitors. The measurements were carried out in the potential range from 0 to 1 V. Figure 5 shows the charge/discharge behavior of capacitors at a constant current density of 2.5 mA cm^{-2} . On the basis of the different capacitances of the supercapacitors, the charge and discharge phases last different times. The electric efficiency was higher than 96% for the studied carbon-based supercapacitors, indicating a high charge/discharge propagation, low resistivity, and good reversible process.^{16,35} The

(33) Andreas, H. A.; Conway, B. E. *Electrochim. Acta* **2006**, *51*, 6510–6520.

(34) Peters, D. G. In *Organic Electrochemistry*, 4th ed.; Lund, H., Hammerich, O., Eds.; Marcel Dekker, Inc.: New York, 2001; pp 341–377.

(35) Mitani, S.; Lee, S. I.; Saito, K.; Korai, Y.; Mochida, I. *Electrochim. Acta* **2006**, *51*, 5487–5493.

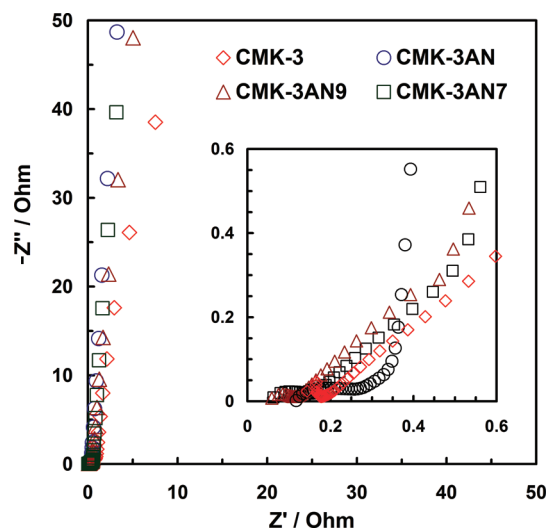


Figure 6. Nyquist plot of different supercapacitors based on carbons CMK-3, CMK-3AN, CMK-3AN7, and CMK-3AN9. The inset shows the high-frequency region of impedance.

voltage drop (iR) related to the internal resistance^{1,36} is very low for these capacitors and is practically invisible in the curves during the changing of polarity from the negative to positive current and vice versa. However, because the software of the instrument was not specifically developed to calculate the iR drop, we were unable to measure the resistance this way.

3.4. EIS Studies of Carbon-Based Supercapacitors. EIS is an important analytical technique used to gain information about the characteristic frequency responses of supercapacitors and the capacitive phenomena occurring in the composite electrodes.

The Nyquist impedance plots of the different carbon-based supercapacitors are reported in Figure 6. The inset in the figure shows the impedance behavior at high frequencies of the capacitors. The impedance behavior shows for some capacitors a loop at a high frequency that is likely to be because of the charge-transfer process and/or the different contact resistances.^{1,19} Observing the plots at lower frequencies (mHz), the points depict shapes close to those of ideal capacitors. At high frequencies, the resistance characteristics of the different supercapacitors are expressed by the so-called electric series resistance (ESR), which includes electrolyte resistance, collector/electrode contact resistance, and the resistance of the electrode/electrolyte interface. For the studied supercapacitors, the values of ESR were 0.45, 0.55, 0.73, and $0.70 \Omega \text{ cm}^2$ for CMK-3AN9, CMK-3AN7, CMK-3, and CMK-3AN, respectively. The ESR of the supercapacitor with the CMK-3AN carbon in the electrodes was higher than that of thermal-treated carbons because it had a lower degree of graphitization and higher content of oxygen-containing functional groups, as shown in Table 2, which negatively influence the electronic conductivity of the material, but it has one advantage for improving the carbon and electrode wettability. Moreover, the surface functional groups, in the CMK-3AN sample, supply additional electric charges by pseudo-capacitive processes because of their redox reactions. The distortion of the rectangular shape of the curves that showed the carbons CMK-3AN and CMK-3

(36) Hulicova-Jurcakova, D.; Li, X.; Zhu, Z.; De Marco, R.; Lu, G. Q. *Energy Fuels* **2008**, *22*, 4139–4145.

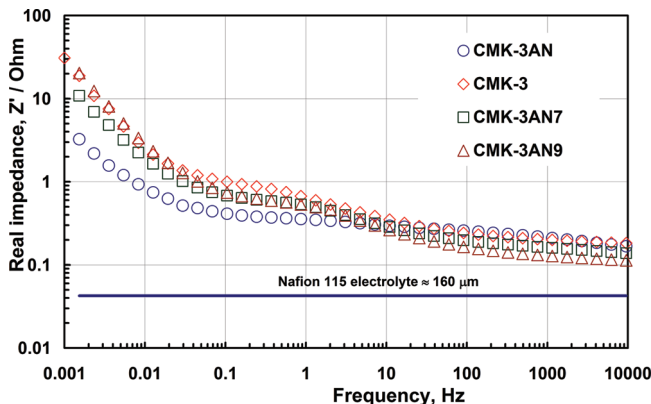


Figure 7. Real impedance (Z' , resistance) behavior as a function of the frequency of the carbon-based supercapacitors. The straight line in the lower region of the figure represents the resistance of the Nafion 115 electrolyte $\approx 160 \mu\text{m}$

(Figure 4) for voltages less than 0.3 V in the charge/discharge phase is a clear demonstration of the presence of these processes. Although pseudo-capacitance behavior is not clearly visible in the shape of curves of Figure 4 for the CMK-3AN7 and CMK-3AN9 carbon electrodes, a relatively high content of oxygen (3.66 and 4.11%) indicates that these materials also exhibit pseudo-capacitance from the redox process even if at a less extent than CMK-3 and CMK-3AN carbons. A rough estimation of values of capacitance for the CMK-3 and CMK-3AN carbons compared to thermal-treated samples (CMK-3AN7 and CMK-3AN9) demonstrates that the pseudo-capacitance could be higher than 300% of the double-layer capacitance even if it cannot be quantified with precision.

Figure 7 shows the behavior of the real component of impedance as a function of the frequency of the different capacitors. Initially, in the high-frequency region, the value of impedance is ascribed to resistance of the Nafion electrolyte,³⁷ indicated in the figure with a parallel straight line at a resistance of 0.042Ω . To this, the carbon electrodes, interfaces, and contacts between electrodes and current collector resistances are added.

A higher content of oxygen-containing functional groups present on the surface is found for unmodified carbon (CMK-3) and nitric-acid-treated carbon (CMK-3AN) compared to those of the thermal-treated carbons (CMK-3AN7 and CMK-3AN9) and have, as an advantage, an improved transport of ions in smaller carbon pores on the basis of less hydrophobic characteristics,³⁸ as observed from the resistance behavior shown in Figure 7 for the CMK-3AN carbon-based capacitor. Figure 7 shows that, at a high frequency, the main resistance of carbon-based supercapacitors is of the electronic type (together with that ionic of the electrolyte), but in the middle range of the frequency (≈ 2 – 100 Hz), the ionic resistance, which is derived from the ion penetration into pores, becomes comparable to the electronic resistance. However, at frequencies lower than 1 Hz, the ionic transport prevails and controls the total resistance. This resistance behavior is well-explained by the CMK-3AN carbon, which has a high electronic resistance at a high frequency because of a lower graphitic character than thermal-treated carbons

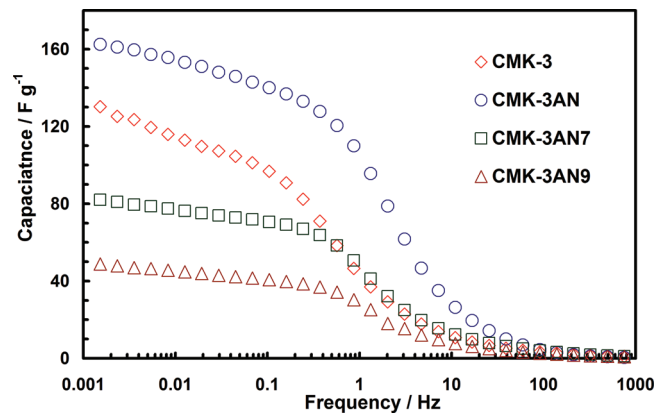


Figure 8. Specific capacitance (F g^{-1}) of the carbon-based supercapacitors as a function of the frequency. The capacitance is normalized for the weight of active carbon materials for one electrode.

(CMK-3AN7 and CMK-3AN9), whereas in the middle range of frequencies, it has a resistance comparable to other carbon materials. The situation changes at lower frequencies (in the region of mHz), where a lower ionic resistance because of an enhanced transport of ions of CMK-3AN than other carbons is present.

Figure 8 shows the capacitance behavior as a function of the frequency for the different supercapacitors. At a low frequency of 1 mHz, the values of capacitance were 162, 130, 82, and 49 F g^{-1} for CMK-3AN, CMK-3, CMK-3AN7, and CMK-3AN9 EL, respectively, and the normalized capacitance (per unit of surface area) was $21.1, 20.5, 13.0$, and $8.3 \mu\text{F cm}^{-2}$ for the same carbons. The analysis of these results indicates clearly that the capacitance of CMK-3AN and CMK-3 is mainly owed to the pseudo-capacitance from the faradaic process and that only a small fraction of capacitance is purely capacitive. The porous properties do not seem to influence the performance because of similar characteristics of modified and unmodified template carbons.

The capacitance performance of these template carbon-based solid-state supercapacitors, which achieved a value of 162 F g^{-1} for the CMK-3AN-based supercapacitor, was higher than that reported by Zhou et al.³⁹ for the same type of CMK-3 carbon, measured in a three-electrode cell using LiPF₆/ethylene carbonate (EC) as the electrolyte/solvent. The capacitances reported by Zhou et al.³⁹ varied from 60 to 90 F g^{-1} , whereas another study by Vix-Guterl et al.²⁷ reported values of capacitance of 167 and 93 F g^{-1} in 1 M H₂SO₄ and Et₄NBF₄, respectively.

It is well-known from the literature that values of specific capacitances of 150 – 200 F g^{-1} are generally obtained in aqueous electrolyte supercapacitors, whereas values of 80 – 120 F g^{-1} are achieved in non-aqueous electrolytes.^{1–3,40} The former type of capacitors have the advantage of higher power density, whereas with non-aqueous organic electrolytes, a higher energy density ($E_{\max} = 1/2\text{CV}^2$) is achieved because of the wide voltage window (up to ≈ 2.5 V). However, this study, in which mesoporous carbons were used in solid-state supercapacitors, is a new subject in this field, and we highlight the advantages of this technology in the design and development of lightweight and flexible devices.

(37) Lufrano, F.; Staiti, P.; Minutoli, M. *J. Electrochem. Soc.* **2004**, 151, A64–A68.

(38) Kwon, T.; Nishihara, H.; Itoi, H.; Yang, Q.-H.; Kyotani, T. *Langmuir* **2009**, 25, 11961–11968.

(39) Zhou, H.; Zhu, S.; Hibino, M.; Honma, I. *J. Power Sources* **2003**, 122, 219–223.

(40) Lota, G.; Centeno, T. A.; Frackowiak, E.; Stoeckli, F. *Electrochim. Acta* **2008**, 53, 2210–2216.

One finding of this work is that potential improvements of supercapacitor features could be achieved by (a) increasing the specific surface area and optimizing the pore structures of mesoporous carbons, (b) adding oxygen-containing functional groups on carbon surfaces, and (c) increasing the knowledge of the ionic transport through pores and wettability of electrodes.

However, because there are various influences, for example, between oxygen-containing functional groups and pore structures, an easy correlation between the capacitance derived from non-faradaic and faradaic processes is unobtainable for these carbon materials. Nevertheless, if you compare the specific capacitance of CMK-3AN and CMK-3 ($\approx 21 \mu\text{F cm}^{-2}$) to that of the CMK-3AN9 carbon ($8.3 \mu\text{F cm}^{-2}$), a higher value by about 250% for the former is found. This increase of capacitance is attributable to pseudo-capacitance because of the faradaic process for the presence of quinone-type oxygen groups on the carbon surface, especially for CMK-3AN and CMK-3 carbons.

4. Conclusion

A mesoporous carbon material was synthesized using the silica SBA-15 as a template. The synthesized carbon (CMK-3) showed an ordered mesoporous structure with a pore diameter

of about 3.5 nm. The CMK-3 carbon was successively chemically modified by a nitric acid treatment (CMK-3AN), and different oxygen-containing functional groups were inserted onto the carbon surfaces. Two other samples, CMK-3AN7 and CMK-3AN9, were prepared from the CMK-3AN carbon by successive thermal treatment at 700 and 900 °C, respectively, and in these carbons, the functionalities were partially removed.

A series of composite electrodes was prepared with the different mesoporous carbons, CMK-3, CMK-3AN, CMK-3AN7, and CMK-3AN9, and used in solid-state supercapacitors. The highest specific capacitance was obtained with the CMK-3AN carbon (162 F g^{-1}), whereas that of the untreated CMK-3 carbon was of 130 F g^{-1} , and those of CMK-3AN7 and CMK-3AN9 were 82 and 49 F g^{-1} , respectively. The high performances of the CMK-3AN and CMK-3 carbons were demonstrated to be governed from pseudo-capacitance because of the different content of oxygenated groups on the surface of the carbons rather than their specific surface area and porous properties. Specifically, the study also showed that the pseudo-capacitance was attributed to electrochemically active functionalities, such as quinone groups. Other oxygen groups could be electrochemically active to provide pseudo-capacitance, but these were not well-recognized in this study and neither well-demonstrated in the literature.